

Photoluminescence study of excitons in homoepitaxial GaN

G. Martínez-Criado^{a)}

Materials Science Institute and Department of Applied Physics, University of Valencia, Dr. Moliner 50, 46100-Burjasot, Valencia, Spain

C. R. Miskys

Walter Schottky Institute, Technical University Munich, Am Coulombwall, 85748-Garching, Germany

A. Cros

Materials Science Institute and Department of Applied Physics, University of Valencia, Dr. Moliner 50, 46100-Burjasot, Valencia, Spain

O. Ambacher

Walter Schottky Institute, Technical University Munich, Am Coulombwall, 85748-Garching, Germany

A. Cantarero

Materials Science Institute and Department of Applied Physics, University of Valencia, Dr. Moliner 50, 46100-Burjasot, Valencia, Spain

M. Stutzmann

Walter Schottky Institute, Technical University Munich, Am Coulombwall, 85748-Garching, Germany

(Received 27 June 2001; accepted for publication 28 August 2001)

High-resolution photoluminescence spectra have been measured in high-quality homoepitaxial GaN grown on a free-standing GaN substrate with lower residual strain than in previous work. Unusually strong and well-resolved excitonic lines were observed. Based on free- and bound exciton transitions some important GaN parameters are derived. The Arrhenius plot of the free A exciton recombination yields a binding energy of 24.7 meV. Based on this datum, an accurate value for the band-gap energy, $E_G(4.3 \text{ K}) = 3.506 \text{ eV}$, can be given. From the donor bound excitons and their "two-electron" satellites, the exciton localization energy and donor ionization energy are deduced. Finally, estimates of the electron and hole masses have been obtained within the effective mass approximation. © 2001 American Institute of Physics. [DOI: 10.1063/1.1413713]

I. INTRODUCTION

Although intense research efforts have been aimed at understanding the optical properties of GaN, important intrinsic parameters such as the electronic band gap, free-exciton binding energy, effective masses, impurity ionization energies, etc., remain controversial or poorly known.^{1,2} The scatter in the data published up to now is due to the strong influence of residual strain caused by the mismatch of lattice constants and thermal expansion coefficients between thin epitaxial GaN films and substrates, and high background impurity concentration, giving rise to broad and badly resolved photoluminescence (PL) spectra. Unwanted impurities and/or electric fields produced by a random distribution of ionized impurities substantially contribute to the inhomogeneous broadening of electronic states, to the extent that the resulting line shapes are insufficient for an accurate determination of the above-mentioned parameters by optical measurements. Most optical studies published so far have been concerned with the origin of the deep yellow band,^{3,4} impurity bound-exciton recombination,^{5,6} or other shallow donor-acceptor pair emissions.⁷

Recently, progress has been made in the homoepitaxial growth of GaN films on free-standing and bulk GaN

substrates.^{8,9} The availability of high-quality GaN layers with low background impurity concentration and dislocation density enables the accurate study of free- and bound exciton transitions without the presence of any strain. Here, we discuss high-resolution PL measurements of a high-quality homoepitaxial GaN layer, which has an exceptionally low lattice mismatch around 3×10^{-5} , a dislocation density of $2 \times 10^7 \text{ cm}^{-2}$, and a free-carrier concentration of $5 \times 10^{16} \text{ cm}^{-3}$ at room temperature.

II. EXPERIMENT

Samples were grown by metal-organic chemical-vapor-phase deposition (MOCVD) on free-standing high-quality GaN substrates obtained by a laser-induced lift-off process of 300- μm -thick films grown by hydride vapor-phase epitaxy (HVPE) on sapphire. A more detailed description of the MOCVD and HVPE growth conditions, as well as an exhaustive structural characterization of the sample used in the present study, can be found in Ref. 8 and are summarized in Table I.

For the PL measurements the sample was mounted in a continuous He-flow cryostat. The precision of the temperature determination is $\pm 1 \text{ K}$. For optical excitation the 333.6 nm line of the Ar^+ laser was used. The laser power incident normally on the sample surface was $70 \mu\text{W}$, and was focused with a $10\times$ microscope objective to a spot diameter of ~ 8

^{a)}Electronic mail: gmc@uv.es

TABLE I. Summary of relevant structural and electrical parameters of both substrate and layer.^a

Parameters	GaN substrate	GaN layer
Thickness (μm)	300	2
Lattice mismatch (%)	...	<0.003
Dislocation density (cm^{-2})	2×10^7	2×10^7
Free-carrier concentration at 300 K (cm^{-3})	8×10^{15}	5×10^{16}
Hall mobility at 300 K ($\text{cm}^2/\text{V s}$)	350	310

^aReference 8.

μm . The luminescence light was detected with a 0.8 m DILOR triple-grating spectrometer equipped with a cooled charge-coupled-device (CCD) detector. This experimental setup allows a spectral resolution better than 0.12 meV (1 cm^{-1}) at $\lambda = 333.6 \text{ nm}$.

III. RESULTS AND DISCUSSION

The PL spectrum at 4.3 K for the homoepitaxial GaN film is shown in Fig. 1 on a linear scale. Several lines are visible, which have been identified as the free A exciton recombination (X_A) at 3.4810 eV, the neutral donor bound exciton transitions (D_1^0-X) and (D_2^0-X), at 3.4788 and 3.4745 eV, respectively, and the acceptor bound-exciton line (A^0-X) at 3.4691 eV. The recombination of the free B exciton (X_B) is shown on the expanded linear scale above the X_A line at 3.4870 eV. Additionally, the so-called “two-electron” transition ($(D_2^0-X)_{n=2}$) emerges at 3.4530 eV when the donor is left in an excited $2s$ -like state.¹⁰ The assignment that we have made is based on the thermal and excitation power dependencies of the PL lines which are discussed below. The acquired spectrum is typical of a nominally undoped GaN layer with residual impurities; the very good crystal quality of the sample is proved by the donor bound exciton linewidth of $500 \mu\text{eV}$, and also the presence of well-resolved excitonic lines. As expected, the bound exciton transitions are narrower than the corresponding free-exciton recombination lines because the exciton localization reduces

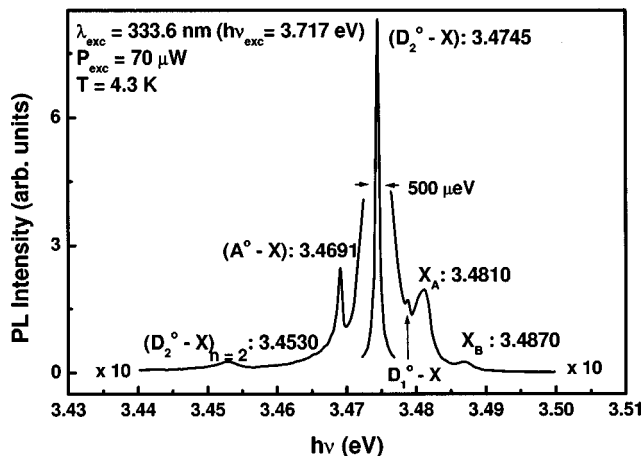


FIG. 1. Photoluminescence spectrum from a high-quality homoepitaxial film measured at 4.3 K with an exciting power of $\sim 70 \mu\text{W}$. The attribution of spectral lines to transitions involving excitons and shallow donors and acceptors is indicated.

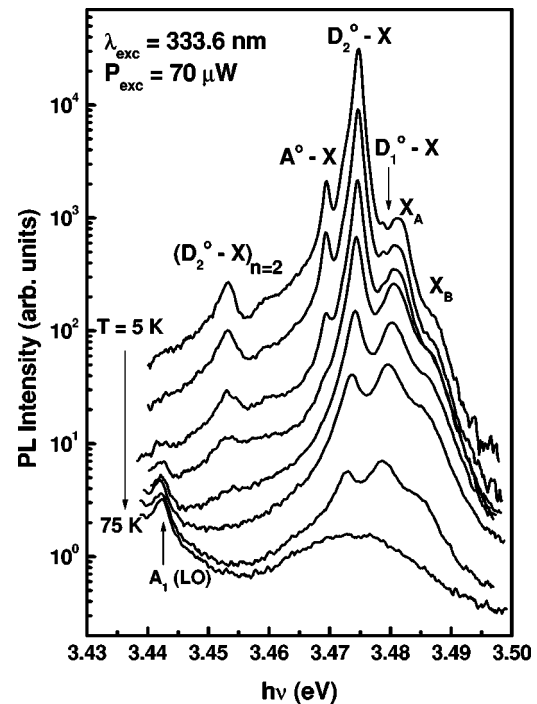


FIG. 2. Temperature dependence of the photoluminescence spectra.

the broadening due to impurities, disorder, defects, and thermal energy. Similar linewidths have been reported earlier for GaN homoepitaxial films grown by MOCVD and molecular-beam epitaxy (MBE) on bulk GaN substrates.^{11,12} However, the energy positions of the donor bound exciton transition for those samples (3.469 and 3.471 eV) are not in agreement with our value, indicating different residual strain. This small difference can be related to the significantly higher carrier concentrations in the bulk GaN substrates ($\sim 5 \times 10^{19} \text{ cm}^{-3}$) (Ref. 13) than the epitaxial layers ($\sim 10^{17}$), being their lattice constants different and resulting in a mismatch of $\Delta a/a \approx 2 \times 10^{-4}$, an order of magnitude larger than our samples.⁸ Therefore, in order to evaluate accurate fundamental optical parameters, the lattice mismatch must be negligible. Nevertheless, from a technological point of view bulk GaN substrates are more attractive at present than free-standing substrates since they offer a noticeable lower dislocation density ($10^2 - 10^4 \text{ cm}^{-2}$) in spite of being highly conductive.¹³

An essential remark is the thermal behavior of the PL spectrum shown in Fig. 2 together with the $3A_1(\text{LO})$ Raman emission. When the temperature increases the PL features change smoothly but significantly in contrast to the Raman signal. Between 5 and 55 K, the higher energy peaks, X_A and X_B , broaden and become relatively stronger, turning into the dominant recombination processes consistent with a free-exciton nature. The weakening and quenching of the bound exciton recombinations, ($D_{1,2}^0-X$) and (A^0-X), is observed due to thermal dissociation of the respective complexes. Naturally, the (D_2^0-X)_{n=2} line quenches faster with temperature than the main (D_2^0-X) peak. All of these spectra were fitted using a multi-Gaussian fitting procedure in order to obtain an accurate determination of each PL peak energy and relative intensity of the different recombination channels. As the temperature increases, the dominant shift in the

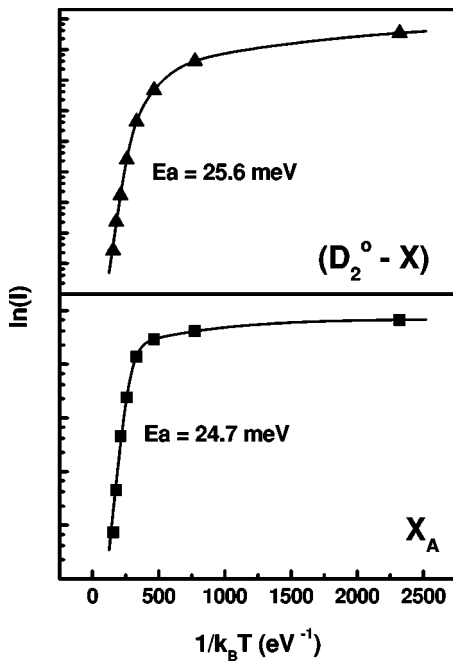


FIG. 3. Arrhenius plots of the integrated intensities vs $1/k_B T$ for the free A exciton (X_A) and neutral donor bound exciton transitions ($D_2^0 - X$). Solid curves represent theoretical fits to Eq. (1).

exciton peak positions is in agreement with the band-gap shrinkage of h -GaN,¹⁴ excepting the energy offset due to different residual strains. Figure 3 shows the natural logarithm of the integrated intensity of the the A free-exciton line versus $1/k_B T$. In general, two different temperature regimes can be distinguished: at very low temperatures, up to 35 K, the intensity remains constant, with a very low activation energy E_1 . Above this value, a very rapid quenching is observed, indicating the free-exciton dissociation. An analysis of these data has been carried out using the well-known thermal activation relation:¹⁵

$$I = \frac{A}{1 + \sum_i B_i e^{-E_i/k_B T}} \quad (1)$$

A detailed evaluation shows that two activation energies are sufficient for a satisfactory fit of X_A . The respective activation energies obtained from the fitting procedure are given in Table II. The functions with the parameters obtained from the fit provide curves which describe the data points with a reliable approximation.

Adding the free A exciton binding energy deduced from the Arrhenius plot, $E_X = 24.7$ meV, to the energetic position

TABLE II. Activation energies are shown for the free A exciton (X_A) and neutral donor bound exciton transitions ($D_2^0 - X$) obtained from Eq. (1). The energy positions ($h\nu$) of these emissions are also listed.

Transition	$h\nu$ (eV)	E_1 (meV)	E_2 (meV)	E_3 (meV)	B_1	B_2	B_3	A
X_A	3.4810	1.8	...	24.7	1.02	...	1.6×10^3	2.33
$D_2^0 - X$	3.4745	1.4	7.2	25.6	5.12	244.5	1.6×10^3	41.63

centered at 3.4810 eV, we obtain for the band-gap energy 3.5057 eV for the strain-free GaN at 4.3 K. Moreover, from the difference of the free A exciton and donor bound exciton energies, the exciton localization energy, E_{BX} , i.e., the energy required to remove the exciton from the neutral donor, can be easily deduced:

$$h\nu_{(D_2^0 - X)} = E_G - E_X - E_{BX} = h\nu_{X_A} - E_{BX} \quad (2)$$

The obtained value, $E_{BX} = 6.5$ meV, agrees within experimental uncertainty with the activation energy of $E_2 = 7.2$ meV obtained in the second region of the donor bound exciton thermal quenching, corroborating the exciton dissociation from the donor center (see Fig. 3). Evidently, the corresponding free-exciton dissociation takes place next with an activation energy $E_3 = 25.6$ meV.

In the same way, the “two-electron” transition ($D_2^0 - X$) _{$n=2$} can be used to obtain information about the neutral donor binding energy, E_D . For this case, the exciton recombines and the neutral donor returns to the ground state, or it may pick up energy from the exciton, leaving eventually the electron on the donor in an excited state. The energy of this transition is then:

$$h\nu_{(D_2^0 - X)_{n=2}} = E_G - E_X - E_{BX} - \Delta E = h\nu_{(D_2^0 - X)} - \Delta E \quad (3)$$

where ΔE is the energy necessary to put the donor into its first excited state. From these energies, a donor binding energy of 28.6 meV has been derived assuming the energy level sequence of a hydrogen atom ($\Delta E = 3/4 E_D$). Such a donor binding energy has been attributed to silicon atoms on gallium sites.¹ Our value is slightly lower than the 31.7 meV obtained by Volm *et al.*¹⁶ using their measured localization energy and the Haynes rule,¹⁷ and is very close to the 29 meV in a moderately doped sample determined by Wang *et al.*¹⁸ from an extrapolation of their magnetic-field dependence of infrared absorption to zero field. Given the respective uncertainties in the determination of these values in the published experiments, our result for the ionization energy of the Si donor is a good compromise. In the effective mass approximation the donor impurity induces a shallow hydrogenic state tied to the conduction-band bottom whose binding energy is given by

$$E_D = \frac{m_e e^4}{2\hbar^2 \epsilon_0^2} = \frac{m_e R_H}{m_0 \epsilon_0^2} \quad (4)$$

where R_H is the Rydberg constant. Therefore, with $\epsilon_0 = 9.5$,¹⁹ the electron effective mass is estimated to $0.19m_0$, close to $0.22m_0$, the value obtained by electron cyclotron resonance experiments in MOVPE GaN.²⁰ Actually, wurtzite GaN is a hexagonal crystal with axial symmetry. The effective mass equation for hydrogenic states should, in principle, be modified because the reduced effective masses as well as the dielectric constant are anisotropic. However, it has been demonstrated that, to a good approximation, the isotropic reduced masses and dielectric constant are still valid approaches.¹⁹ Hence, the effective hole mass m_h can be derived from the free A exciton binding energy:

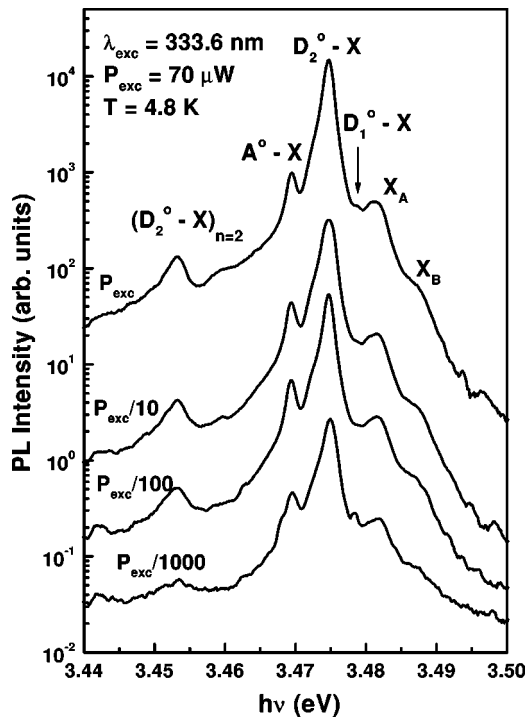


FIG. 4. Variation of the photoluminescence spectra with excitation power density at 4.8 K.

$$E_X = \frac{\mu e^4}{2\hbar^2 \epsilon_0^2} = \frac{R_H}{m_0 \epsilon_0^2} \left(\frac{1}{m_e} + \frac{1}{m_h} \right)^{-1}. \quad (5)$$

We obtain $m_h = 1.19m_0$, which matches within 10% to another experimental determination by PL and two-photon spectroscopy ($m_h = 1.2m_0$) (Ref. 21) and first-principles calculations ($m_h = 1.10m_0$).²²

It is important to notice that for the spectral resolution used in our experiment the donor bound exciton transition was not a single line; two transitions ($D_1^0 - X$, $D_2^0 - X$) are clearly resolved and separated by approximately 4 meV. This peculiarity is not only typical of our sample, but also arises in other GaN films.^{16,23} The transition could result from two independent donor bound exciton lines, which likewise entail the coexistence of two shallow donors. Alternative mechanisms are excited states of either the donor or the exciton. The observation of donor excited states is improbable since the energy separation should be 3/4 of the effective Rydberg, $E_D = 28.6$ meV, too large to explain our results. On the other hand, an excited state of the neutral donor bound exciton would also be 3/4 of the binding energy in the effective mass approximation. Therefore, taking the binding energy of 25.8 meV, the first excited state should appear around 20 meV above the ground state. Finally, the possibility that the two lines originate from donor bound excitons relating to A and B valence bands can be ruled out because their energy separation is also larger than 4 meV.¹ For all of these reasons, we have labeled the two transitions in question as coming from two different residual donors; however, this point needs to be investigated further.

In order to obtain further information on the origin of these PL lines, we have recorded the PL spectrum for various

excitation intensities, spanning a dynamic range of three decades (see Fig. 4). All lines do not show any shift with intensity, consistent with an exciton origin. The integrated intensities for each transition increases nonlinearly with the excitation power. By using a power-law dependence of luminescence intensity I on the excitation power P , $I \propto P^n$, values of $n \geq 1.4$ are obtained for all lines. This behavior corroborates their excitonic nature as opposed to other recombination mechanisms.²⁴ Since the rate of the exciton formation depends on the product of the electron and hole densities, the exciton PL emission is expected to be superlinear in excitation power.

IV. CONCLUSIONS

In summary, very narrow and well-resolved spectral excitonic structures have been observed in a high-quality homoepitaxial GaN film. Strong free and donor bound exciton recombinations enable us to accurately determine the transition energies and to identify the excitonic nature of the PL lines, allowing a precise evaluation of the band-gap energy. Within the framework of the effective mass approximation, we were able to perform a straightforward estimate of the A free binding energy, the ionization energy of the residual donor, as well as the electron and hole effective masses characteristic for high-quality GaN.

ACKNOWLEDGMENTS

One of the authors (G.M.-C.) would like to thank the Agencia Española de Cooperación Internacional (AECI) for granting her fellowship, as well as the Generalitat Valenciana for continuous support. In the same way, A.C. gratefully acknowledges financial support under Grant Nos. GV00-080-15 and MAT2000-0772.

¹N. E. Christensen and P. Perlin, in *Gallium Nitride I*, edited by J. I. Pankove and T. D. Moustakas, Semiconductors and Semimetals Series (Academic, New York, 1998), Vol. 50.

²H. Morkoç in *Nitride Semi-conductors and Devices*, edited by R. Hull, R. M. Osgood, Jr., H. Sakaki, and A. Zunger, Springer Series in Materials Science (Springer, Berlin, 1999), Vol. 32.

³E. Calleja, F. J. Sánchez, D. Basak, M. A. Sánchez-García, E. Muñoz, I. Izpura, F. Calle, J. M. G. Tijero, and J. L. Sánchez-Rojas, *Phys. Rev. B* **55**, 4689 (1997).

⁴L. W. Tu, Y. C. Lee, D. Stocker, and E. F. Schubert, *Phys. Rev. B* **58**, 10696 (1998).

⁵G. Martínez-Criado, A. Cros, A. Cantarero, R. Dimitrov, O. Ambacher, and M. Stutzmann, *J. Appl. Phys.* **88**, 3470 (2000).

⁶P. W. Yu, C. S. Park, and S. T. Kim, *J. Appl. Phys.* **89**, 1692 (2001).

⁷E. M. Goldys, M. Godlewski, R. Langer, A. Barski, P. Bergman, and B. Monemar, *Phys. Rev. B* **60**, 5464 (1998).

⁸C. R. Miskys, M. K. Kelly, O. Ambacher, G. Martínez-Criado, and M. Stutzmann, *Appl. Phys. Lett.* **77**, 1858 (2000).

⁹M. Schauler, F. Eberhard, C. Kirchner, V. Schwegler, A. Pelzmann, M. Kamp, K. J. Ebeling, F. Bertram, T. Riemann, J. Christen, P. Prystawko, M. Leszczynski, I. Grzegory, and S. Porowski, *Appl. Phys. Lett.* **74**, 1123 (1999).

¹⁰L. Pavesi and M. Guzzi, *J. Appl. Phys.* **75**, 4779 (1994).

¹¹Z. X. Liu, K. P. Korona, K. Syassen, J. Kuhl, K. Pakula, J. M. Baranowski, I. Grzegory, and S. Porowski, *Solid State Commun.* **108**, 433 (1998).

¹²T. Talliercio, M. Gallart, P. Lefebvre, A. Morel, B. Gil, J. Allègre, N. Grandjean, J. Massies, I. Grzegory, and S. Porowski, *Solid State Commun.* **117**, 445 (2001).

¹³I. Grzegory and S. Porowski, *Thin Solid Films* **367**, 281 (2000).

¹⁴F. Calle, F. J. Sánchez, J. M. G. Tijero, M. A. Sánchez-García, E. Calleja,

- and R. Beresford, *Semicond. Sci. Technol.* **12**, 1396 (1997).
- ¹⁵D. Bimberg, M. Sondergeld, and E. Grobe, *Phys. Rev. B* **4**, 3451 (1971).
- ¹⁶D. Volm, K. Oettinger, T. Streibl, D. Kovalev, M. Ben-Chorin, J. Diener, B. K. Meyer, J. Majewski, L. Eeckey, and A. Hoffmann, *Phys. Rev. B* **53**, 16543 (1996).
- ¹⁷J. R. Haynes, *Phys. Rev. Lett.* **4**, 351 (1960).
- ¹⁸Y. J. Wang, R. Kaplan, H. K. Ng, K. Doverspike, D. K. Gaskill, T. Ikedo, I. Akasaki, and H. Amono, *J. Appl. Phys.* **79**, 8007 (1996).
- ¹⁹W. Shan, B. D. Little, A. J. Fischer, J. J. Song, B. Goldenberg, W. G. Perry, M. D. Bremser, and R. F. Davis, *Phys. Rev. B* **54**, 16369 (1996).
- ²⁰M. Drechsler, D. M. Hofmann, B. K. Meyer, T. Detchprohm, H. Amano, and I. Akasaki, *Jpn. J. Appl. Phys., Part 2* **34**, L1178 (1995).
- ²¹K. Reimann, M. Steube, D. Fröhlich, and S. J. Clarke, *J. Cryst. Growth* **189/190**, 652 (1998).
- ²²M. Suzuki, T. Uenoyama, and A. Yanase, *Phys. Rev. B* **52**, 8132 (1995).
- ²³B. J. Skromme, J. Jayapalan, R. P. Vaudo, and V. M. Phanse, *Appl. Phys. Lett.* **74**, 2358 (1999).
- ²⁴T. Schmidt, K. Lischka, and W. Zulehner, *Phys. Rev. B* **45**, 8989 (1992).